Three-Dimensional Quantitative Structure−Property Relationship (3D-QSPR) Models for Prediction of Thermodynamic Properties of Polychlorinated Biphenyls (PCBs): Enthalpy of Vaporization

Swati Puri, James S. Chickos, and William J. Welsh*,†

Department of Chemistry and Biochemistry and Center for Molecular Electronics, University of Missouri−St. Louis, 8001 Natural Bridge Road, St. Louis, Missouri 63121

Received August 31, 2001

Three-dimensional Quantitative Structure−Property Relationship (QSPR) models have been derived using Comparative Molecular Field Analysis (CoMFA) to correlate the vaporization enthalpies of a representative set of polychlorinated biphenyls (PCBs) at 298.15 K with their CoMFA-calculated physicochemical properties. Various alignment schemes, such as *inertial*, *as is*, and *atom fit*, were employed in this study. The CoMFA models were also developed using different partial charge formalisms, namely, electrostatic potential (ESP) charges and Gasteiger−Marsili (GM) charges. The most predictive model for vaporization enthalpy ($\Delta_{vap}H_m$(298.15 K)), with *atom fit* alignment and Gasteiger−Marsili charges, yielded r^2 values 0.852 (cross-validated) and 0.996 (conventional). The vaporization enthalpies of PCBs increased with the number of chlorine atoms and were found to be larger for the meta- and para-substituted isomers. This model was used to predict $\Delta_{vap}H_m$(298.15 K) of the entire set of 209 PCB congeners.

INTRODUCTION

Since the atmosphere is a significant pathway for the transport of organic pollutants, considerable effort has been expended for the measurement of physicochemical properties that govern the movement of chemicals in the environment. Polychlorinated biphenyls (PCBs) are persistent organic contaminants that are found at an appreciable concentration in the polar region, presumably as a result of long-range atmospheric transport.[1] For many environmental applications, the subcooled liquid vapor pressures and vaporization enthalpies are the relevant thermodynamic properties associated with the dispersal of PCBs.[2,3]

Gas chromatography has been frequently used to determine vapor pressures and subsequently, the vaporization enthalpies of PCBs.[4,5] In the work reported by Bidleman, the standard compounds used were octadecane for more volatile PCBs and eicosane for less volatile PCBs.[4] The value used by Bidleman for the vaporization enthalpy of octadecane was 84.5 kJ/mol at 340 K; the value used for eicosane was 93.4 kJ/mol at 362 K. The vaporization enthalpies of these two standard compounds at 340 and 362 K, respectively, were used to calculate the vaporization enthalpies of 32 PCBs at 298.15 K.[5] Recently, Ruzicka and Majer[6] have recommended the following vaporization enthalpies at 298.15 K for octadecane and eicosane:

$$\text{octadecane } \Delta_{vap}H_m\,(298.15\text{ K}) = 91.4\text{ kJ/mol}$$

$$\text{eicosane } \Delta_{vap}H_m\,(298.15\text{ K}) = 101.8\text{ kJ/mol}$$

A comparison of the recommended values of $\Delta_{vap}H_m$ at 298.15 and 340 K reveals a difference of approximately 7 kJ/mol for octadecane. A difference of 8 kJ/mol was observed in the value of $\Delta_{vap}H_m$ for eicosane at 298.15 and 362 K. In view of the large discrepancies in the recommended values at 298.15 K and the values used by Bidleman, we decided to reexamine the vaporization enthalpies of a representative set of PCBs using the technique of correlation gas chromatography.[7] The vaporization enthalpies of PCBs determined in our study[7] are considerably larger than the values originally cited by Falconer and Bidleman.[5] However, if the enthalpies for octadecane and eicosane at 298.15 K are used to correct the vaporization enthalpies of PCBs reported by Falconer and Bidleman,[5] the results are in good agreement with the values determined by our study.[7]

Several computational techniques have been developed and applied to evaluate the relationship between gas chromatographic retention behavior and descriptors such as molecular polarizabilities,[8] ionization potentials,[8,9] degree of chlorination,[9,10] substitution pattern of PCBs,[10] and solvent accessible surface area.[11] This is a successful yet complex approach since the molecular descriptors must be calculated to derive these relationships.

Comparative Molecular Field Analysis (CoMFA)[12] is generally regarded as the industry standard for constructing three-dimensional quantitative structure−activity relationship (3D-QSAR) models. It is based on the observation that most intermolecular interactions are shape-dependent and noncovalent.[12] Vaporization enthalpy is a thermodynamic property that depends on the strength of the intermolecular interactions. This study aims to develop simple and predictive models that establish a correlation between the vaporization enthalpies at 298.15 K ($\Delta_{vap}H_m$(298.15 K)) and the CoMFA-generated steric and electrostatic fields surrounding the PCB molecules.

* Corresponding author phone: (732)235-5313; fax: (732)235-4073; e-mail: welshwj@umdnj.edu.

† Current address: Department of Pharmacology, Robert Wood Johnson Medical School, University of Medicine & Dentistry of New Jersey, 675 Hoes Lane, Piscataway, NJ 08854-5635.

10.1021/ci010093j CCC: $22.00
Published on Web 00/00/0000 PAGE EST: 5.4

Alignment Schemes. This study investigates different alignment schemes and partial charge formalisms for the development of predictive models for the vaporization enthalpies of PCBs at 298.15 K. *Atom fit* alignment of molecules performs a least-squares fit between two molecules by matching pairs of atoms. The quality of the fit is denoted by the root-mean-square distance (RMSD) value computed for the matched atoms.[13] The *as is* option in the *Database Align* module in SYBYL 6.7 molecular modeling software (Tripos, Inc., St. Louis, MO) does not change the orientation of the molecules. *Inertial* alignment of PCBs to the biphenyl template, in which only carbon atoms of the biphenyl ring were considered for alignment, was also performed in SYBYL. Partial atomic charges derived from both the calculated electrostatic potential (ESP),[14] and Gasteiger−Marsili (GM)[15] methods have been used in conjunction with *atom fit* alignment of molecules.

METHODOLOGY

The molecular modeling and CoMFA computations were performed on a Silicon Graphics Inc. (SGI) Indy workstation running the IRIX (version 6.2) operating system. The molecules in the data set were constructed using SYBYL 6.7 molecular modeling software (Tripos, Inc., St. Louis, MO). All molecules were geometry optimized by implementing the Merck Molecular Force Field (MMFF94)[16] with a distance dependent dielectric function ($\epsilon = \epsilon_o r$, with $\epsilon_o = 1$) until the convergence criterion of 0.004184 kJ/mol (0.001 kcal/mol) change in energy between successive iterations was achieved.

Three semiempirical methods, namely, MNDO (Modified Neglect of Diatomic Overlap),[17] PM3 (Parametric Method 3),[18] and AM1 (Austin Model 1),[19] have been reviewed in the literature to calculate the rotational barriers and preferred conformations of biphenyl.[20] Mulholland et al.[20] found that AM1 is the most reliable method to estimate the optimum dihedral angle and rotational energy barriers, with results comparable to experimental observations and ab initio calculations. Consequently, the optimized structures from SYBYL were used as initial coordinates for AM1 geometry optimization in SPARTAN (Version 5.0.1, Wavefunction, Inc., Irvine, CA). The conformational space about the twist bond connecting the two ring systems was systematically explored from 0° to 360° in 25 steps (i.e., 14.4° increments). The lowest energy conformer obtained from this search was subjected to AM1 geometry optimization. Partial atomic charges were computed using the electrostatic potential (ESP)[14] utility in SPARTAN.

Data Set. The data set of 17 compounds consisted of a biphenyl molecule and 16 PCBs. The vaporization enthalpies of these compounds at 298.15 K have been determined by the authors using correlation gas chromatography,[7] and these values were used to develop the CoMFA models in this study. This data set was divided into a training set of 15 compounds and a test set of two PCBs. The test set generally comprises about 10% of the total number of compounds in the data set. Isomers 15 (4,4′-dichlorobiphenyl) and 95 (2,2′,3,5′,6-pentachlorobiphenyl) were selected as the test set since these compounds are representative of the dichlorobiphenyl and pentachlorobiphenyl homologues .

Alignment Schemes. Biphenyl was selected as the template molecule for various alignment schemes in this study.

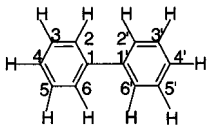

Figure 1. Atoms C1, C2, C4, and C5 of the biphenyl template were selected for *atom fit* alignment of PCB molecules.

For *atom fit* alignment, PCB molecules were aligned via RMSD fit of carbon atoms C1, C2, C4, and C5 to the corresponding atoms on the biphenyl ring (Figure 1). These atoms were selected to consider the *ortho* (C2), *meta* (C5), and *para* (C4) positions on the benzene ring, and the atom (C1) connected to the carbon atom of the second benzene ring.

Inertial and *as is* alignment schemes were also used to align PCB compounds to the biphenyl template. *Atom fit* alignment was used to study the effect of partial atomic charges on the vaporization enthalpy of PCBs. The ESP charges were imported from SPARTAN and Gasteiger−Marsili (GM) charges were computed in SYBYL.

After alignment of the compounds in the data set, each PCB molecule was placed in the center of a regularly spaced grid of 2.0 Å dimensions in x, y, and z directions. The steric (van der Waals/Lennard-Jones 12−6 function) and electrostatic (Coulomb's Law function) potential energy fields were calculated separately at each grid point of the three-dimensional lattice by summing the individual energy interactions between each atom of the PCB molecule and a probe consisting of a sp^3 hybridized carbon atom with +1 charge. A distance-dependent dielectric function was applied, and values of the steric and electrostatic energies were truncated at 125 kJ/mol.

Partial Least Squares (PLS) Analysis. Partial least squares (PLS)[21] is a regression technique that expresses a dependent variable (target property) in terms of linear combinations of the independent variables (descriptor data). All calculations were performed using the QSAR module in SYBYL. The QSPR table was constructed with rows containing values of $\Delta_{vap}H_m$(298.15 K) of each compound in the training set as the dependent variable. The columns contained the steric and electrostatic fields as the independent variables.

The predictive ability of the CoMFA models was examined using the "leave-one-out" cross-validation procedure, in which each compound is systematically excluded from the data set and its property predicted by a model that is derived from the remaining compounds. The PLS analysis with cross-validation yields an optimum number of principal components (PCs, also called latent variables), which are associated with the highest cross-validated r^2 (r_{cv}^2) value. The PLS analysis was repeated without cross-validation using the optimum number of components. This procedure yielded a predictive model and associated conventional r^2 values.

RESULTS AND DISCUSSION

The statistical results of the CoMFA analysis using different alignment schemes and partial charge formalisms are summarized in Table 1. There are three models that demonstrate excellent internal predictive ability for the vaporization enthalpy of PCBs at 298.15 K: *atom fit*

Table 1. Summary of Statistical Results from CoMFA-PLS Analysis of Vaporization Enthalpies ($\Delta_{vap}H_m$(298.15 K)) of 15 PCBs in the Training Set Using Different Alignment Schemes and Partial Charge Formalisms

alignment scheme partial charge formalism	*atom fit* ESP[a]	*atom fit* GM[b]	*inertial* ESP[a]	*as is* ESP[a]
cross-validated r^2 (r_{cv}^2)	0.734 (0.769)	0.812 (0.852)	0.673 (0.689)	0.862 (0.764)
conventional r^2	0.987 (0.981)	0.998 (0.996)	0.896 (0.921)	0.995 (0.992)
standard error of estimate	2.06 (2.22)	0.857 (1.06)	4.97 (4.21)	1.30 (1.48)
principal components	5 (5)	6 (6)	2 (3)	6 (6)
F values	132 (115)	642 (427)	51.4 (50.2)	280 (219)

[a] Electrostatic potential. [b] Gasteiger−Marsili. [c] The values in parentheses represent the statistical results for the original data set of 17 PCBs.

Table 2. Comparison of Experimental and CoMFA-Predicted Values (*Atom Fit* Alignment, GM Charges) of Vaporization Enthalpy ($\Delta_{vap}H_m$(298.15 K) in kJ/mol) for the Model Constructed Using the Original Data Set of 17 PCBs

IUPAC no.	compounds	exptl	pred	residual[a]
	biphenyl	64.5	64.9	−0.4
1	2-monochlorobiphenyl	72.1	72.1	0.0
2	3-monochlorobiphenyl	74.3	74.7	−0.4
3	4-monochlorobiphenyl	71.6	69.7	1.9
7	2,4-dichlorobiphenyl	75.4	74.8	0.6
9	2,5-dichlorobiphenyl	76.8	77.9	−1.1
11	3,3′-dichlorobiphenyl	81.0	80.9	0.1
15	4,4′-dichlorobiphenyl	81.4	82.2	−0.8
18	2,2′,5-trichlorobiphenyl	80.2	81.5	−1.3
49	2,2′,4,5′-tetrachlorobiphenyl	87.4	87.0	0.4
53	2,2′,5,6′- tetrachlorobiphenyl	84.9	85.1	−0.2
95	2,2′,3,5′,6-pentachlorobiphenyl	92.3	92.1	0.2
96	2,2′,3,6,6′- pentachlorobiphenyl	89.6	87.9	1.7
103	2,2′,4,5′,6- pentachlorobiphenyl	91.6	92.1	−0.5
153	2,2′,4,4′,5,5′-hexachlorobiphenyl	103.5	103.4	0.1
156	2,3,3′,4,4′,5-hexachlorobiphenyl	112.6	112.1	0.5
171	2,2′,3,3′,4,4′,6-heptachlorobiphenyl	109.1	109.4	−0.3

[a] The residual is the difference between experimental and CoMFA-predicted values of vaporization enthalpy ($\Delta_{vap}H_m$(298.15 K)).

alignment with ESP charges, *atom fit* alignment with GM charges, and *as is* alignment scheme with ESP charges.

The model that combined *atom fit* alignment and GM charges demonstrated exceptional self-consistency (r^2 = 0.998) and internal predictive ability (r_{cv}^2 = 0.812). This model, which consists of 15 PCBs in the training set, required six PCs to explain the variation in $\Delta_{vap}H_m$(298.15 K) values. The model was used to predict $\Delta_{vap}H_m$(298.15 K) of the two test-set compounds. The CoMFA-predicted value of $\Delta_{vap}H_m$(298.15 K) was 81.8 kJ/mol (experimental value = 81.4 kJ/mol) for isomer 15 and 92.1 kJ/mol (experimental value = 92.3 kJ/mol) for isomer 95.

The two compounds in the test set were added to the training set and this model, which now consisted of 17 PCBs, was used to predict $\Delta_{vap}H_m$(298.15 K) values of the remaining 193 PCBs. Details of the CoMFA study of $\Delta_{vap}H_m$(298.15 K) using *atom fit* alignment and GM charges for the data set of 17 PCBs are given in Table 2. This model exhibited a strong correlation between experimental and CoMFA-predicted values of vaporization enthalpies of PCBs at 298.15 K (Figure 2). The model constructed with *atom fit* alignment and GM charges for the data set comprising 17 PCBs, with cross-validated r^2 (r_{cv}^2) value of 0.852 and conventional r^2 value of 0.996, was used to predict the $\Delta_{vap}H_m$(298.15 K) values of the remaining 193 PCB isomers for which experimental vaporization enthalpies are not available in the literature to the best of our knowledge (Table 3).

The vaporization enthalpy of PCBs tends to increase as the total number of chlorine atoms on the biphenyl ring

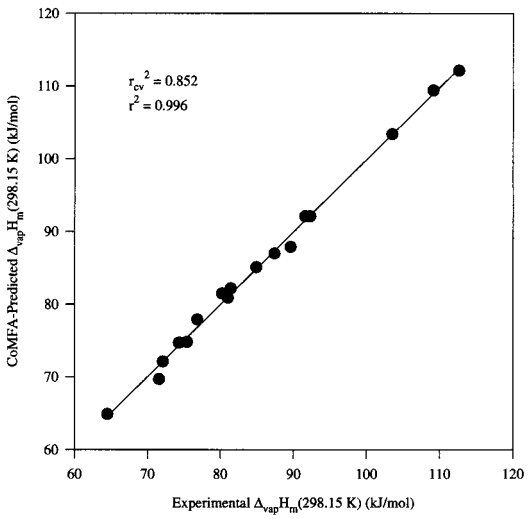

Figure 2. A plot of CoMFA-predicted (*atom fit* alignment, GM charges) versus experimental values of vaporization enthalpies ($\Delta_{vap}H_m$(298.15 K)) for the 17 PCBs in the original data set.

increases (Table 4) yet tends to decrease as the number of ortho-chlorine atoms increases. The enthalpies are generally higher for the meta- and para-substituted PCBs than for the corresponding ortho-substituted isomers, presumably since the former can more easily adopt the coplanar conformation. Coplanar molecules can stack more efficiently, resulting in stronger intermolecular steric (van der Waals) interactions. This will result in lowered vapor pressure and increased enthalpy of vaporization. These factors will also increase as a function of molecular size.

The above observations can be illustrated by citing examples within the pentachlorobiphenyl homolog. The vaporization enthalpies of isomers 95 (2,2′,3,5′,6-pentachlorobiphenyl) and 103 (2,2′,4,5′,6-pentachlorobiphenyl) are nearly equal at 92.3 and 91.6 kJ/mol, respectively (Table 2). However, the vaporization enthalpy of isomer 96 (2,2′,3,6,6′-pentachlorobiphenyl) is distinctly lower at 89.6 kJ/mol. Isomer 96 has four ortho chlorine atoms compared to three ortho chlorine atoms on isomers 95 and 103. Comparison of other homologues shows the same general trend. For example, the vaporization enthalpy is higher for isomer 156 (2,3,3′,4,4′,5-hexachlorobiphenyl) at 112.6 kJ/mol than for isomer 153 (2,2′,4,4′,5,5′-hexachlorobiphenyl) at 103.5 kJ/mol and for isomer 171 (2,2′,3,3′,4,4′,6-heptachlorobiphenyl) at 109.1 kJ/mol. Note that isomer 156 contains only one ortho-Cl atom, whereas isomers 153 and 171 contain two and three ortho-Cl atoms, respectively.

CONCLUSIONS

This study represents a successful extension of CoMFA into the realm of three-dimensional quantitative structure−

Table 3. CoMFA-Predicted Values of Vaporization Enthalpy ($\Delta_{vap}H_m$(298.15 K) in kJ/mol) for 193 PCBs in the Test Set, Using the Model (*Atom Fit* Alignment, Gasteiger−Marsili Charges) Constructed from the Original Data Set of 17 PCBs

IUPAC no.	compounds	no. of atoms: Cl	no. of atoms: ortho Cl	CoMFA pred values	IUPAC no.	compounds	no. of atoms: Cl	no. of atoms: ortho Cl	CoMFA pred values
4	2,2′-dichlorobiphenyl	2	2	72.6	86	2,2′,3,4,5-pentachlorobiphenyl	5	2	93.1
5	2,3-dichlorobiphenyl	2	1	73.4	87	2,2′,3,4,5′-pentachlorobiphenyl	5	2	99.6
6	2,3′-dichlorobiphenyl	2	1	77.8	88	2,2′,3,4,6-pentachlorobiphenyl	5	3	89.0
8	2,4′-dichlorobiphenyl	2	1	76.5	89	2,2′,3,4,6′-pentachlorobiphenyl	5	3	88.6
10	2,6-dichlorobiphenyl	2	2	80.6	90	2,2′,3,4′,5-pentachlorobiphenyl	5	2	96.0
12	3,4-dichlorobiphenyl	2	0	79.5	91	2,2′,3,4′,6-pentachlorobiphenyl	5	3	89.2
13	3,4′-dichlorobiphenyl	2	0	82.0	92	2,2′,3,5,5′-pentachlorobiphenyl	5	2	97.0
14	3,5-dichlorobiphenyl	2	0	81.4	93	2,2′,3,5,6-pentachlorobiphenyl	5	3	88.5
16	2,2′,3-trichlorobiphenyl	3	2	79.9	94	2,2′,3,5,6′-pentachlorobiphenyl	5	3	88.1
17	2,2′,4-trichlorobiphenyl	3	2	81.6	97	2,2′,3′,4,5-pentachlorobiphenyl	5	2	96.3
19	2,2′,6-trichlorobiphenyl	3	3	81.0	98	2,2′,3′,4,6-pentachlorobiphenyl	5	3	96.3
20	2,3,3′-trichlorobiphenyl	3	1	93.7	99	2,2′,4,4′,5-pentachlorobiphenyl	5	2	102.3
21	2,3,4-trichlorobiphenyl	3	1	88.6	100	2,2′,4,4′,6-pentachlorobiphenyl	5	3	92.1
22	2,3,4′-trichlorobiphenyl	3	1	81.0	101	2,2′,4,5,5′-pentachlorobiphenyl	5	2	95.6
23	2,3,5-trichlorobiphenyl	3	1	90.1	102	2,2′,4,5,6′-pentachlorobiphenyl	5	3	88.4
24	2,3,6-trichlorobiphenyl	3	2	89.2	104	2,2′,4,6,6′-pentachlorobiphenyl	5	4	86.3
25	2,3′,4-trichlorobiphenyl	3	1	93.2	105	2,3,3′,4,4′-pentachlorobiphenyl	5	1	106.7
26	2,3′,5-trichlorobiphenyl	3	1	89.4	106	2,3,3′,4,5-pentachlorobiphenyl	5	1	106.9
27	2,3′,6-trichlorobiphenyl	3	2	80.7	107	2,3,3′,4′,5-pentachlorobiphenyl	5	1	102.2
28	2,4,4′-trichlorobiphenyl	3	1	89.3	108	2,3,3′,4,5′-pentachlorobiphenyl	5	1	100.9
29	2,4,5-trichlorobiphenyl	3	1	82.9	109	2,3,3′,4,6-pentachlorobiphenyl	5	2	95.2
30	2,4,6-trichlorobiphenyl	3	2	91.1	110	2,3,3′,4′,6-pentachlorobiphenyl	5	2	97.6
31	2,4′,5-trichlorobiphenyl	3	1	91.2	111	2,3,3′,5,5′-pentachlorobiphenyl	5	1	102.0
32	2,4′,6-trichlorobiphenyl	3	2	82.9	112	2,3,3′,5,6-pentachlorobiphenyl	5	2	94.7
33	2′,3,4-trichlorobiphenyl	3	1	88.3	113	2,3,3′,5′,6-pentachlorobiphenyl	5	2	95.1
34	2′,3,5-trichlorobiphenyl	3	1	83.3	114	2,3,4,4′,5-pentachlorobiphenyl	5	1	107.1
35	3,3′,4-trichlorobiphenyl	3	0	90.1	115	2,3,4,4′,6-pentachlorobiphenyl	5	2	97.4
36	3,3′,5-trichlorobiphenyl	3	0	85.7	116	2,3,4,5,6-pentachlorobiphenyl	5	2	108.0
37	3,4,4′-trichlorobiphenyl	3	0	91.1	117	2,3,4′,5,6-pentachlorobiphenyl	5	2	96.9
38	3,4,5-trichlorobiphenyl	3	0	89.2	118	2,3′,4,4′,5-pentachlorobiphenyl	5	1	107.6
39	3,4′,5-trichlorobiphenyl	3	0	86.8	119	2,3′,4,4′,6-pentachlorobiphenyl	5	2	102.2
40	2,2′,3,3′-tetrachlorobiphenyl	4	2	94.7	120	2,3′,4,5,5′-pentachlorobiphenyl	5	1	106.2
41	2,2′,3,4-tetrachlorobiphenyl	4	2	90.5	121	2,3′,4,5′,6-pentachlorobiphenyl	5	2	99.7
42	2,2′,3,4′-tetrachlorobiphenyl	4	2	95.2	122	2′,3,3′,4,5-pentachlorobiphenyl	5	1	103.7
43	2,2′,3,5-tetrachlorobiphenyl	4	2	86.3	123	2′,3,4,4′,5-pentachlorobiphenyl	5	1	104.4
44	2,2′,3,5′-tetrachlorobiphenyl	4	2	84.4	124	2′,3,4,5,5′-pentachlorobiphenyl	5	1	104.6
45	2,2′,3,6-tetrachlorobiphenyl	4	3	80.5	125	2′,3,4,5,6′-pentachlorobiphenyl	5	2	96.0
46	2,2′,3,6′-tetrachlorobiphenyl	4	3	85.9	126	3,3′,4,4′,5-pentachlorobiphenyl	5	0	107.4
47	2,2′,4,4′-tetrachlorobiphenyl	4	2	90.3	127	3,3′,4,5,5′-pentachlorobiphenyl	5	0	104.4
48	2,2′,4,5-tetrachlorobiphenyl	4	2	90.8	128	2,2′,3,3′,4,4′-hexachlorobiphenyl	6	2	106.0
50	2,2′,4,6-tetrachlorobiphenyl	4	3	81.2	129	2,2′,3,3′,4,5-hexachlorobiphenyl	6	2	99.3
51	2,2′,4,6′-tetrachlorobiphenyl	4	3	86.5	130	2,2′,3,3′,4,5′-hexachlorobiphenyl	6	2	113.2
52	2,2′,5,5′-tetrachlorobiphenyl	4	2	84.5	131	2,2′,3,3′,4,6-hexachlorobiphenyl	6	3	96.6
54	2,2′,6,6′-tetrachlorobiphenyl	4	4	79.4	132	2,2′,3,3′,4,6′-hexachlorobiphenyl	6	3	101.1
55	2,3,3′,4-tetrachlorobiphenyl	4	1	102.8	133	2,2′,3,3′,5,5′-hexachlorobiphenyl	6	2	96.8
56	2,3,3′,4′-tetrachlorobiphenyl	4	1	99.7	134	2,2′,3,3′,5,6-hexachlorobiphenyl	6	3	92.1
57	2,3,3′,5-tetrachlorobiphenyl	4	1	96.1	135	2,2′,3,3′,5,6′-hexachlorobiphenyl	6	3	97.0
58	2,3,3′,5′-tetrachlorobiphenyl	4	1	101.9	136	2,2′,3,3′,6,6′-hexachlorobiphenyl	6	4	94.2
59	2,3,3′,6-tetrachlorobiphenyl	4	2	89.8	137	2,2′,3,4,4′,5-hexachlorobiphenyl	6	2	105.3
60	2,3,4,4′-tetrachlorobiphenyl	4	1	98.6	138	2,2′,3,4,4′,5′-hexachlorobiphenyl	6	2	103.1
61	2,3,4,5-tetrachlorobiphenyl	4	1	93.8	139	2,2′,3,4,4′,6-hexachlorobiphenyl	6	3	102.5
62	2,3,4,6-tetrachlorobiphenyl	4	2	97.6	140	2,2′,3,4,4′,6′-hexachlorobiphenyl	6	3	100.9
63	2,3,4′,5-tetrachlorobiphenyl	4	1	94.1	141	2,2′,3,4,5,5′-hexachlorobiphenyl	6	2	106.2
64	2,3,4′,6-tetrachlorobiphenyl	4	2	91.7	142	2,2′,3,4,5,6-hexachlorobiphenyl	6	3	91.0
65	2,3,5,6-tetrachlorobiphenyl	4	2	97.8	143	2,2′,3,4,5,6′-hexachlorobiphenyl	6	3	94.6
66	2,3′,4,4′-tetrachlorobiphenyl	4	1	93.0	144	2,2′,3,4,5′,6-hexachlorobiphenyl	6	3	96.5
67	2,3′,4,5-tetrachlorobiphenyl	4	1	96.6	145	2,2′,3,4,6,6′-hexachlorobiphenyl	6	4	92.3
68	2,3′,4,5′-tetrachlorobiphenyl	4	1	102.5	146	2,2′,3,4′,5,5′-hexachlorobiphenyl	6	2	106.8
69	2,3′,4,6-tetrachlorobiphenyl	4	2	90.3	147	2,2′,3,4′,5,6-hexachlorobiphenyl	6	3	98.3
70	2,3′,4′,5-tetrachlorobiphenyl	4	1	96.1	148	2,2′,3,4′,5,6′-hexachlorobiphenyl	6	3	96.5
71	2,3′,4′,6-tetrachlorobiphenyl	4	2	92.8	149	2,2′,3,4′,5′,6-hexachlorobiphenyl	6	3	97.1
72	2,3′,5,5′-tetrachlorobiphenyl	4	1	97.8	150	2,2′,3,4′,6,6′-hexachlorobiphenyl	6	4	95.7
73	2,3′,5′,6-tetrachlorobiphenyl	4	2	90.2	151	2,2′,3,5,5′,6-hexachlorobiphenyl	6	3	92.0
74	2,4,4′,5-tetrachlorobiphenyl	4	1	94.4	152	2,2′,3,5,6,6′-hexachlorobiphenyl	6	4	87.8
75	2,4,4′,6-tetrachlorobiphenyl	4	2	92.4	154	2,2′,4,4′,5,6′-hexachlorobiphenyl	6	3	96.9
76	2′,3,4,5-tetrachlorobiphenyl	4	1	92.4	155	2,2′,4,4′,6,6′-hexachlorobiphenyl	6	4	96.3
77	3,3′,4,4′-tetrachlorobiphenyl	4	0	97.8	157	2,3,3′,4,4′,5′-hexachlorobiphenyl	6	1	117.0
78	3,3′,4,5-tetrachlorobiphenyl	4	0	94.8	158	2,3,3′,4,4′,6-hexachlorobiphenyl	6	2	110.7
79	3,3′,4,5′-tetrachlorobiphenyl	4	0	99.7	159	2,3,3′,4,5,5′-hexachlorobiphenyl	6	1	111.4
80	3,3′,5,5′-tetrachlorobiphenyl	4	0	95.3	160	2,3,3′,4,5,6-hexachlorobiphenyl	6	2	103.5
81	3,4,4′,5-tetrachlorobiphenyl	4	0	95.8	161	2,3,3′,4,5′,6-hexachlorobiphenyl	6	2	108.4
82	2,2′,3,3′,4-pentachlorobiphenyl	5	2	92.5	162	2,3,3′,4′,5,5′-hexachlorobiphenyl	6	1	112.6
83	2,2′,3,3′,5-pentachlorobiphenyl	5	2	91.7	163	2,3,3′,4′,5,6-hexachlorobiphenyl	6	2	106.7
84	2,2′,3,3′,6-pentachlorobiphenyl	5	3	89.2	164	2,3,3′,4′,5′,6-hexachlorobiphenyl	6	2	111.3
85	2,2′,3,4,4′-pentachlorobiphenyl	5	2	100.2	165	2,3,3′,5,5′,6-hexachlorobiphenyl	6	2	104.2

Table 3 (Continued)

IUPAC no.	compounds	no. of atoms Cl	no. of atoms ortho Cl	CoMFA pred values	IUPAC no.	compounds	no. of atoms Cl	no. of atoms ortho Cl	CoMFA pred values
166	2,3,4,4′,5,6-hexachlorobiphenyl	6	2	106.0	189	2,3,3′,4,4′,5,5′-heptachlorobiphenyl	7	1	122.1
167	2,3′,4,4′,5,5′-hexachlorobiphenyl	6	1	112.2	190	2,3,3′,4,4′,5,6-heptachlorobiphenyl	7	2	115.7
168	2,3′,4,4′,5′,6-hexachlorobiphenyl	6	2	112.0	191	2,3,3′,4,4′,5′,6-heptachlorobiphenyl	7	2	120.5
169	3,3′,4,4′,5,5′-hexachlorobiphenyl	6	0	112.0	192	2,3,3′,4,5,5′,6-heptachlorobiphenyl	7	2	113.5
170	2,2′,3,3′,4,4′,5-heptachlorobiphenyl	7	2	116.0	193	2,3,3′,4′,5,5′,6-heptachlorobiphenyl	7	2	113.2
172	2,2′,3,3′,4,5,5′-heptachlorobiphenyl	7	2	117.2	194	2,2′,3,3′,4,4′,5,5′-octachlorobiphenyl	8	2	119.6
173	2,2′,3,3′,4,5,6-heptachlorobiphenyl	7	3	99.6	195	2,2′,3,3′,4,4′,5,6-octachlorobiphenyl	8	3	117.3
174	2,2′,3,3′,4,5,6′-heptachlorobiphenyl	7	3	103.3	196	2,2′,3,3′,4,4′,5,6′-octachlorobiphenyl	8	3	111.4
175	2,2′,3,3′,4,5′,6-heptachlorobiphenyl	7	3	114.3	197	2,2′,3,3′,4,4′,6,6′-octachlorobiphenyl	8	4	110.5
176	2,2′,3,3′,4,6,6′-heptachlorobiphenyl	7	4	100.8	198	2,2′,3,3′,4,5,5′,6-octachlorobiphenyl	8	3	108.1
177	2,2′,3,3′,4′,5,6-heptachlorobiphenyl	7	3	102.9	199	2,2′,3,3′,4,5,5′,6′-octachlorobiphenyl	8	3	112.1
178	2,2′,3,3′,5,5′,6-heptachlorobiphenyl	7	3	105.5	200	2,2′,3,3′,4,5,6,6′-octachlorobiphenyl	8	4	102.8
179	2,2′,3,3′,5,6,6′-heptachlorobiphenyl	7	4	96.3	201	2,2′,3,3′,4,5′,6,6′-octachlorobiphenyl	8	4	109.2
180	2,2′,3,4,4′,5,5′-heptachlorobiphenyl	7	2	111.9	202	2,2′,3,3′,5,5′,6,6′-octachlorobiphenyl	8	4	104.7
181	2,2′,3,4,4′,5,6-heptachlorobiphenyl	7	3	102.0	203	2,2′,3,4,4′,5,5′,6-octachlorobiphenyl	8	3	110.7
182	2,2′,3,4,4′,5,6′-heptachlorobiphenyl	7	3	102.8	204	2,2′,3,4,4′,5,6,6′-octachlorobiphenyl	8	4	104.4
183	2,2′,3,4,4′,5′,6-heptachlorobiphenyl	7	3	113.1	205	2,3,3′,4,4′,5,5′,6-octachlorobiphenyl	8	2	125.5
184	2,2′,3,4,4′,6,6′-heptachlorobiphenyl	7	4	102.2	206	2,2′,3,3′,4,4′,5,5′,6-nonachlorobiphenyl	9	3	119.0
185	2,2′,3,4,5,5′,6-heptachlorobiphenyl	7	3	99.6	207	2,2′,3,3′,4,4′,5,6,6′-nonachlorobiphenyl	9	4	115.4
186	2,2′,3,4,5,6,6′-heptachlorobiphenyl	7	4	94.5	208	2,2′,3,3′,4,5,5′,6,6′-nonachlorobiphenyl	9	4	114.9
187	2,2′,3,4′,5,5′,6-heptachlorobiphenyl	7	3	106.0	209	2,2′,3,3′,4,4′,5,5′,6,6′-decachlorobiphenyl	10	4	121.4
188	2,2′,3,4′,5,6,6′-heptachlorobiphenyl	7	4	97.9					

Table 4. Average Values of CoMFA-Predicted[a] $\Delta_{vap}H_m$(298.15 K) for the Entire Set of 209 PCBs Grouped by Homologue (Number of Chlorine Atoms) and Number of Ortho-Chlorine Atoms

	average $\Delta_{vap}H_m$(298.15 K), kJ/mol				
total no. of Cl atoms	0[b]	1[b]	2[b]	3[b]	4[b]
2	81.2	76.1	76.6	-	-
3	88.6	88.3	83.8	81.0	-
4	96.7	97.1	91.0	83.8	79.4
5	105.9	104.8	97.4	90.3	87.1
6	112.0	113.1	106.1	96.7	93.3
7		122.1	115.4	105.3	98.3
8			122.6	111.9	106.3

[a] The CoMFA model (*atom fit* alignment, GM charges) corresponds to the original data set of 17 PCBs. Note the general trend that the vaporization enthalpies tend to increase as the total number of chlorine atoms increases but to decrease with increasing number of ortho-chlorine atoms. [b] Number of ortho-Cl atoms.

property relationship (3D-QSPR) models by constructing simple and predictive models for the vaporization enthalpies of PCBs at 298.15 K. The combination of *atom fit* alignment and Gasteiger−Marsili charges yielded a statistically robust model ($r_{cv}^2 = 0.852$; $r^2 = 0.996$), and this model was used to predict $\Delta_{vap}H_m$(298.15 K) of the entire set of 209 PCB congeners.

Similar 3D-QSPR models can be derived for the vaporization enthalpies of other organic compounds, such as polychlorinated dibenzo-p-dioxins, which belong to the same class of persistent organic pollutants as polychlorinated biphenyls. The data from this study will influence the estimation of other important physicochemical properties of PCBs, for example, heats of partitioning. The techniques developed in this study can also be used to model vapor pressures and octanol/air partition coefficients, important parameters that influence estimation of mass transport in the atmosphere. The enthalpies of vaporization of PCBs predicted in this study should provide some insight into the nature of the fractionation that may occur during the bioaccumulation of organic contaminants in the environment; the vaporization enthalpies of ortho-substituted PCBs are lower, suggesting different migration rates than the corresponding meta and para-substituted isomers.

ACKNOWLEDGMENT

The authors gratefully acknowledge Dr. T. F. Bidleman for his gift of polychlorinated biphenyls. W.J.W. acknowledges the financial support for this research from the U.S. Environmental Protection Agency's Science to Achieve Results (STAR) program. Although the research described in this article has been funded in part by the U.S. Environmental Protection Agency's Science to Achieve Results (STAR) program through grant GAD R826133, it has not been subjected to any EPA review and therefore, does not necessarily reflect the views of the Agency, and no official endorsement should be inferred.

REFERENCES AND NOTES

(1) Wania, F.; Mackay, D. Global Fractionation and Cold Condensation of Low Volatility Organochlorine Compounds in Polar Regions. *AMBIO* **1993**, *22*, 10−18.
(2) Yamasaki, H.; Kuwata, K.; Miyamoto, H. Effects of Ambient Temperature on Aspects of Airborne Polycyclic Aromatic Hydrocarbons. *Environ. Sci. Technol.* **1982**, *16*, 189−194.
(3) Allen, J. O.; Sarofim, A. S.; Smith, K. A. Thermodynamic Properties of Polycyclic Aromatic Hydrocarbons in the Subcooled Liquid State. *Polym. Arom. Compds.* **1999**, *13*, 261−283.
(4) Bidleman, T. F. Estimation of Vapor Pressures for Nonpolar Organic Compounds by Capillary Gas Chromatography. *Anal. Chem.* **1984**, *56*, 2490−2496.
(5) Falconer, R. L.; Bidleman, T. F. Vapor Pressures and Predicted Particle/Gas Distributions of Polychlorinated Biphenyl Congeners as Functions of Temperature and Ortho-Chlorine Substitution. *Atm. Environ.* **1994**, *28*, 547−554.
(6) Ruzicka, K.; Majer, V. Simultaneous Treatment of Vapor Pressures and Related Thermal Data Between the Triple and Normal Boiling Temperatures for *n*-Alkanes C5−C20. *J. Phys. Chem. Ref. Data* **1994**, *23*, 1−39.
(7) Puri, S.; Chickos, J. S.; Welsh, W. J. Determination of Vaporization Enthalpies of Polychlorinated Biphenyls by Correlation Gas Chromatography. *Anal. Chem.* **2001**, *73*, 1480−1484.
(8) Ong, Y. S.; Hites, R. A. Relationship between Gas Chromatographic Retention Indexes and Computer-Calculated Physical Properties of Four Compound Classes. *Anal. Chem.* **1991**, *63*, 2829−2834.
(9) Makino, M.; Kamiya, M.; Matsushita, H. Computer-Assisted Prediction of Gas Chromatographic Retention Times of Polychlorinated Biphenyls by Use of Quantum Chemical Molecular Properties. *Chemosphere* **1992**, *25*, 1839−1849.

(10) Hasan, M. N.; Jurs, P. C. Computer-Assisted Prediction of Gas Chromatographic Retention Times of Polychlorinated Biphenyls. *Anal. Chem.* **1988**, *60*, 978−982.
(11) Makino, M. Novel Classification to Predict Relative Gas Chromatographic Retention Times and *n*-Octanol/Water Partition Coefficients of Polychlorinated Biphenyls. *Chemosphere* **1999**, *39*, 893−903.
(12) Cramer, R. D., III.; Patterson, D. E.; Bunce, J. D. Comparative Molecular Field Analysis (CoMFA). 1. Effect of Shape on Binding of Steroids to Carrier Proteins. *J. Am. Chem. Soc.* **1988**, *110*, 5959−5967.
(13) *The Tripos Bookshelf Version 4.0*; Tripos: St. Louis, MO, 1999; p 9.
(14) (a) Cox, S. R.; Williams, D. E. Representation of the Molecular Electrostatic Potential by a New Atomic Charge Model. *J. Comput. Chem.* **1981**, *2*, 304−323. (b) Chirlian, L. E.; Francl, M. M. Atomic Charges Derived from Electrostatic Potentials: A Detailed Study. *J. Comput. Chem.* **1987**, *8*, 894−905. (c) Breneman, C. M.; Wiberg, K. B. Determining Atom-Centered Monopoles from Molecular Electrostatic Potentials. The Need for High Sampling Density in Formamide Conformational Analysis. *J. Comput. Chem.* **1990**, *11*, 361−373. (d) Singh, U. C.; Kollman, P. A. An Approach to Computing Electrostatic Charges for Molecules. *J. Comput. Chem.* **1984**, *5*, 129−145.] (e) Besler, B. H.; Merz, K. M.; Kollman, P. A. Atomic Charges Derived from Semiempirical Methods. *J. Comput. Chem.* **1990**, *11*, 431−439.
(15) Gasteiger, J.; Marsili, M. Iterative Partial Equalization of Orbital Electronegativity-A Rapid Access to Atomic Charges. *Tetrahedron* **1980**, *36*, 3219−3288.
(16) Halgren, T. A. Merck Molecular Force Field. I. Basis, Form, Scope, Parametrization, and Performance of MMFF94. *J. Comput. Chem.* **1996**, *17*, 490−519.
(17) (a) Dewar, M. J. S.; Thiel, W. Ground States of Molecules. 38. The MNDO Methodol. Approximations and Parameters. *J. Am. Chem. Soc.* **1977**, *99*, 4899−4907. (b) Dewar, M. J. S.; Thiel, W. Ground States of Molecules. 39. MNDO Results for Molecules Containing Hydrogen, Carbon, Nitrogen and Oxygen. *J. Am. Chem. Soc.* **1977**, *99*, 4907−4917.
(18) (a) Stewart, J. J. P. Optimisation of Parameters for Semiempirical Methods I. Methodol. *J. Comput. Chem.* **1989**, *10*, 209−220. (b) Stewart, J. J. P. Optimisation of Parameters for Semiempirical Methods II. Applications. *J. Comput. Chem.* **1989**, *10*, 221−264.
(19) Dewar, M. J. S.; Zoebisch, E. G.; Healy, E. F.; Stewart, J. J. P. AM1: A New General Purpose Quantum Mechanical Model. *J. Am. Chem. Soc.* **1985**, *107*, 3902−3909.
(20) Mulholland, J. A.; Sarofim, A. F.; Rutledge, G. C. Semiempirical Molecular Orbital Estimation of the Relative Stability of Polychlorinated Biphenyl Isomers produced by *o*-Dichlorobenzene Pyrolysis. *J. Phys. Chem.* **1993**, *97*, 6890−6896.
(21) (a) Wold, H. Soft Modeling. The Basic Design and Some Extensions. In *Systems Under* Indirect *Observation: Causality, Structure, Prediction*; Joreskog, K. G., Wold, H., Eds.; Elsevier Science Publishers: Amsterdam, 1982; Vol. II, Chapter 1, p 1. (b) Wold, S.; Albano, C.; Dunn, W. J., III.; Edlund, U.; Esbensen, K.; Geladi, P.; Hellberg, S.; Johansson, E.; Lindberg, W.; Sjosstrom, M. Multivariate Data Analysis in Chemistry. In *Chemometrics: Mathematics and Statistics in Chemistry*; Kowalski, B., Ed.; Reidel: Dordrecht, Netherlands, 1984; pp 17−95.

CI010093J